THE JOURNAL OF BIOLOGICAL CHEMISTRY VOL. 288, NO. 9, pp. 6651–6661, March 1, 2013

Cooperative Recruitment of Dynamin and BIN/Amphiphysin/Rvs (BAR) Domain-containing Proteins Leads to GTP-dependent Membrane Scission*[S]◆

Received for publication, December 13, 2012 Published, JBC Papers in Press, January 7, 2013, DOI 10.1074/jbc.M112.444869

Michael Meinecke[‡§1], Emmanuel Boucrot[‡¶], Gamze Camdere[‡2], Wai-Ching Hon[‡], Rohit Mittal[‡], and Harvey T. McMahon[‡3]

From the [‡]Laboratory of Molecular Biology, Medical Research Council, Hills Road, Cambridge, CB2 0QH, United Kingdom, the [§]Department for Biochemistry II, Georg-August-University Göttingen, 37073 Göttingen, Germany, and [¶]Institute of Structural and Molecular Biology, Division of Biosciences, University College London, London WC1E 6BT, United Kingdom

Background: Dynamin and BAR domain proteins are major components of clathrin-mediated endocytosis and other membrane-trafficking events.
Results: Dynamin is recruited to membranes by BAR domain proteins, which in turn rely on interaction with dynamin to bind membranes.
Conclusion: Membrane binding by dynamin and BAR domain proteins is cooperative and stimulates dynamin and GTP-dependent membrane scission.
Significance: Our results imply synergy of dynamin and BAR domain proteins to promote GTP-dependent vesicle release.

Dynamin mediates various membrane fission events, including the scission of clathrin-coated vesicles. Here, we provide direct evidence for cooperative membrane recruitment of dynamin with the BIN/amphiphysin/Rvs (BAR) proteins, endophilin and amphiphysin. Surprisingly, endophilin and amphiphysin recruitment to membranes was also dependent on binding to dynamin due to auto-inhibition of BAR-membrane interactions. Consistent with reciprocal recruitment *in vitro*, dynamin recruitment to the plasma membrane in cells was strongly reduced by concomitant depletion of endophilin and amphiphysin, and conversely, depletion of dynamin dramatically reduced the recruitment of endophilin. In addition, amphiphysin depletion was observed to severely inhibit clathrin-mediated endocytosis. Furthermore, GTP-dependent membrane scission by dynamin was dramatically elevated by BAR domain proteins. Thus, BAR domain proteins and dynamin act in synergy in membrane recruitment and GTP-dependent vesicle scission.

Clathrin-mediated endocytosis (CME)[4] is a major cellular pathway for synaptic vesicle recycling, receptor internalization, and the uptake of extracellular nutrients (1). It relies on the concerted action of numerous proteins, many of which bind to membranes and sense or induce bilayer morphology changes. BIN/amphiphysin/Rvs (BAR) domain-containing proteins have been proposed to recruit dynamin to the neck regions of forming clathrin-coated pits via their SRC homology 3 (SH3) domains that bind to the C-terminal proline-rich domain (PRD) of dynamin (2–4). They are also implicated in membrane sculpting of the neck regions and thereby forming a template for dynamin oligomerization (5). A mutant of dynamin lacking the PRD remains cytosolic in cells (3) but can still oligomerize *in vitro* on negatively charged membranes (6), suggesting that dynamin oligomerization is facilitated *in vivo* by proteins binding to its PRD. Amphiphysin and endophilin are two prominent contenders. Both have a similar domain organization containing an N-BAR domain and an SH3 domain (7, 8) that binds to the PRD of dynamin (9, 10). In addition, amphiphysin also binds to AP2 and clathrin (11, 12). Overexpression of the amphiphysin SH3 domain inhibits transferrin endocytosis, a defect that can be rescued by overexpression of dynamin but not by an SH3-binding-deficient mutant of dynamin (12, 13). Injection of amphiphysin SH3 domain also inhibits clathrin-coated pit scission in lamprey synapses and in epithelial cells (14, 15).

Endophilin is also implicated in synaptic vesicle retrieval (10, 16–18) and was found to accumulate at the necks of invaginated vesicles in dynamin knock-out (KO) cells (19). In addition, it has been shown that endophilin forms a pre-scission complex with dynamin in lamprey synapses (20). Both amphiphysin and endophilin form complexes with dynamin on membranes (21, 22).

Another protein proposed to be involved in CME is sorting nexin 9 (SNX9) (23, 24). It has a BAR and an SH3 domain that binds to dynamin.

The involvement of BAR domain proteins in dynamin activity is implied from the direct interaction with dynamin (21, 22),

* This work was supported by the Medical Research Council File Reference U105178805, a Human Frontiers Science Program Fellowship (to M. M.), and Deutsche Forschungsgemeinschaft Grant SFB 803 (to M. M.).
◆ This article was selected as a Paper of the Week.
[S] This article contains supplemental Figs. 1 and 2, Movie, and additional references.
[1] To whom correspondence may be addressed: Abteilung Biochemie II, Georg-August-Universität at Göttingen, 37073 Göttingen, Germany. E-mail: michael.meinecke@med.uni-goettingen.de.
[2] Present address: Molecular and Cellular Biology, 408 Barker Hall, University of California at Berkeley, Berkeley, CA 94720-3200.
[3] To whom correspondence may be addressed. E-mail: hmm@mrc-lmb.cam.ac.uk.
[4] The abbreviations used are: CME, clathrin-mediated endocytosis; BAR, BIN/amphiphysin/Rvs; SH3, SRC homology 3; PRD, proline-rich domain; oligo, oligonucleotide; GUV, giant unilamellar vesicle; Tf, transferrin; GTPγS, guanosine 5′-3-*O*-(thio)triphosphate; eGFP, enhanced GFP; PE, phosphatidylethanolamine.

the modulation of dynamin's GTPase activity by these interactions (25, 26), and the coincidence of their recruitment and that of dynamin to sites of vesicle scission (27). However, the role of these BAR domain proteins in dynamin recruitment has remained an inference, which we now investigate.

MATERIALS AND METHODS

Cell Culture, RNAi, and Fixed- and Live-cell Fluorescent Microscopy—SK-MEL-2 DNM2$^{en\text{-}all}$-eGFP and DNM2$^{en\text{-}all}$-eGFP CLTA$^{en\text{-}all}$-RFP genome-edited cells (28) were cultured in DMEM/F-12 Ham's (1:1 v/v), 0.25% sodium bicarbonate (w/v), 1 mM GlutaMAX, and 10% FBS.

Approximately 2×10^5 or 2.5×10^4 cells were cultured on 35-mm glass bottom dishes (MatTek) or 13-mm coverslips, respectively. Cells were transfected twice (on day 1 and 2) with Oligofectamine (Invitrogen) with a total of 80 pmol of each indicated siRNA and analyzed on day 4 (72 h after the first transfection).

The siRNAs used were as follows: Amph1+2 pool 1, HSS100465 (two oligos against human amphiphysin1, Invitrogen) and 4392420 s1341 (one oligo against human amphiphysin2 (BIN1), Ambion); Amph1+2 pool 2, HSS100466 (two oligos against human amphiphysin1, Invitrogen) and 4392420 s1342 (one oligo against human amphiphysin2 (BIN1), Ambion); Amph1+2 pool 3, HSS100467 (two oligos against human amphiphysin1, Invitrogen) and 4392420 s1343 (one oligo against human amphiphysin2 (BIN1), Ambion); EndoA1+2+3 pool 1, L-012597 (four oligos against human endophilinA1, Dharmacon), L-019582 (four oligos against human endophilinA2, Dharmacon), and L-015728 (four oligos against human endophilinA3, Invitrogen); EndoA1+2+3 pool 2, HSS109708 (two oligos against human endophilinA1, Invitrogen), HSS109705 (two oligos against human endophilinA2, Invitrogen), and HSS109711 (two oligos against human endophilinA3, Invitrogen); EndoA1+2+3 pool 3, HSS109709 (two oligos against human endophilinA1, Invitrogen), HSS109706 (two oligos against human endophilinA2, Invitrogen), and HSS109712 (2 oligos against human endophilinA3, Invitrogen); SNX9 siRNA-1, HSS122185 (two oligos against human SNX9, Invitrogen); SNX9 siRNA-2, HSS122186 (two oligos against human SNX9, Invitrogen), SNX9 siRNA-3, HSS122187 (two oligos against human SNX9, Invitrogen); SNX9 pool, HSS122185, HSS122186, and HSS122187 (a total of six oligos against human SNX9, Invitrogen); DNM1+2 pool 1, HSS176208 (two oligos against human dynamin1, Invitrogen) and J-004007-06 (one oligo against human dynamin2, Thermo Scientific); DNM1+2 pool 2, HSS102821 (two oligos against human dynamin1, Invitrogen) and J-004007-08 (one oligo against human dynamin2, Thermo Scientific). Control samples were transfected in the same way as the RNAi samples but a scrambled control siRNA oligo (Invitrogen) was used instead.

In some experiments, cells were transfected using Lipofectamine2000 (Invitrogen) using 0.05 to 0.2 μg or 1 μg (overexpression experiments) of amphiphysin1-eGFP, amphiphysin1-TagRFP-T, amphiphysin2-eGFP, amphiphysin2-TagRFP-T, TagRFP-T-SNX9, endophilinA2-eGFP, or endophilinA2-TagRFP-T (all human). Cells were incubated for 24 h to express the constructs before imaging. Cells were imaged live directly or fixed (3.7% paraformaldehyde, 20 min at room temperature) and stained using goat anti-endophilin (S-15) (sc10880, Santa Cruz Biotechnology), rabbit anti-endophilin (H-60) (sc-25495, Santa Cruz Biotechnology), and donkey anti-goat Alexa-546 or goat anti-rabbit Alexa-546 (Molecular Probes) and mounted on slides using 1,4-diazobicyclo-[2,2,2]-octane. Just before live-cell imaging, the medium was changed to minimum Eagle's medium without phenol red, supplemented with 20 mM HEPES, pH 7.4, and 5% FBS, and placed into a temperature-controlled chamber on the microscope stage with 95% air, 5% CO_2 and 100% humidity. Live-cell imaging was performed as in Ref. 29. Briefly, live-cell and fixed-cell imaging data were acquired using a fully motorized inverted microscope (Eclipse TE-2000, Nikon) equipped with a CSU-X1 spinning disk confocal head (Ultraview Vox, PerkinElmer Life Sciences) using a ×60 lens (Plan Apochromat VC, 1.4 NA, Nikon) under control of Volocity 5.0 (Improvision, UK). 14-Bit digital images were obtained with a cooled EMCCD camera (9100–02, Hamamatsu, Japan). Two 50 milliwatt solid-state lasers (488 and 561; Crystal Laser and Melles Griots) coupled to an individual acoustic-optical tunable filter were used as the light source to excite eGFP and TagRFP-T or Alexa-546 as appropriate.

Dynamin^{en} levels at the plasma membrane (Fig. 1, *B* and *E*) were measured by summing the fluorescence signals on at least 10,000 μm^2 of cell membrane from snapshots at various times along live-cell imaging time lapses. Lifetimes of dynamin^{en} were measured on kymographs. Please note that endogenous dynamin is detected for a longer time than transiently expressed versions (28). Relative levels of BAR domain proteins at the plasma membrane (Fig. 1, *F* and *H*) correspond to the sum of the fluorescence intensities of at least 100 punctae, normalized to the control levels.

Transferrin Uptake and Flow Cytometry—Approximately 1×10^6 RPE1 cells grown in 100-mm dishes were transfected twice (on day 1 and 2) with Oligofectamine (Invitrogen) with a total of 600 pmol of the indicated siRNA and analyzed on day 4 (72 h after the first transfection).

AlexaFluor-488-labeled human transferrin (Molecular Probes, used at 20 μg/ml) uptake was carried at 37 °C for 7 min. Cells were then washed with ice-cold PBS, detached by a 1-min incubation with 0.25% trypsin/EDTA, spun, acid-washed (ice-cold buffer, pH 5, to remove surface-bound ligand), washed, fixed (paraformaldehyde 3.7% for 20 min), washed, and resuspended in PBS and analyzed using LSR II flow cytometer (BD Biosciences). Flow cytometry provided similar phenotypes than those obtained by classical microscopy-based measurement of ligand uptake but allowed an increase in at least 2 log in the number of cells analyzed.

Generation of Giant Unilamellar Vesicles—1-μl drops of lipid mixtures (50 mol % Folch Avanti Polar Lipids (Avanti), 40 mol % Folch Sigma (Sigma), 5 mol % 1-palmitoyl-2-oleoyl-*sn*-glycero-3-phospho-l-serine (Avanti), and 4 mol % phosphatidylinositol 4,5-bisphosphate (Avanti), 1 mo % rhodamine-PE (Avanti)) were applied to indium/tin oxide-covered glass slides. A GUV generation chamber was assembled by separating two slides by a 400 mM glucose solution and thin rubber spacer. We adjusted a previously described electro-formation protocol (30)

so that an electrical field (AC) was applied for 195 min at 55 °C (45 min, 0.1–1.4 V at 10 Hz; 120 min, 1.4 V at 10 Hz; 30 min, 2.1 V at 4.5 Hz). GUVs were freshly prepared for each experiments and used immediately.

Giant Unilamellar Vesicle Assays—Experiments were carried out using the spinning-disc confocal microscope described above. Reactions took place in a 250-μl chamber (Lab-Tek, Borosilicate). To avoid disruption of the GUVs on contact, the chamber was coated with BSA. 50 μl of GUV solution (400 mM sucrose, 20 mM HEPES, pH 7.4) was added to 150 μl of buffer (200 mM NaCl, 20 mM HEPES, pH 7.4). Osmolalities of the GUV solution and the buffer were matched to the osmolalities of the protein solutions. Proteins were added using a 50-μl Hamilton syringe with a bent tip. Protein concentrations are indicated in the figure legends, but these are likely overestimates, as the protein tends to coat the walls of the incubation chamber, as seen from the increasing fluorescent signal. To avoid disruption of the GUVs, the solution was mixed by gentle rotation of a pipette tip. If GTP was used, 100 μM $MgCl_2$ was mixed into the buffer before GUVs were added. All experiments were carried out at 37 °C.

Cloning and Protein Purification—Full-length rat amphiphysin 2–6 and full-length rat endophilin A1 were cloned into pGEX-6P2. Proteins were expressed in BL21 cells for 1 h at 37 °C for amphiphysin and 16 h at 18 °C for the remaining proteins. Cells were lysed using Emulsiflex C3 and spun at 40,000 rpm for 40 min at 4 °C in a Beckman Ti45 rotor, and the supernatant was bound to glutathione beads for 30 min. The beads were washed extensively with 150 mM NaCl, 20 mM HEPES, pH 7.4, 2 mM DTT, 2 mM EDTA, with two washes at 500 mM NaCl in between. The GST tag was cleaved using PreScission protease. Cleaved proteins were further purified by Superdex 200 gel filtration.

Full-length rat dynamin 1 was cloned into pET15b. The SH3 domain of rat amphiphysin 2 (13) was cloned into pGEX-4T2. Proteins were expressed in BL21 cells for 16 h at 18 °C. Cell pellets were mixed in a ratio of 1 liter of amphiphysin SH3 to 6 liters of dynamin. Cells were lysed using Emulsiflex C3 and spun at 125,000 × *g* for 40 min at 4 °C in a Beckman Ti45 rotor, and the supernatant was bound to glutathione beads for 30 min. The beads were washed extensively with 300 mM NaCl, 20 mM Tris, pH 8.5, 2 mM DTT, 2 mM EDTA. Proteins were eluted with free glutathione and bound to Q-Sepharose at 150 mM NaCl and eluted with a salt gradient to 1 M NaCl. Fractions containing dynamin alone were pooled and concentrated. Protein was further purified by Superdex 200 gel filtration.

Dynamin 1 ΔPRD was cloned into pET15b with a PrSc cleavage site after Thr-752. Overexpression and purification were done according to full-length dynamin protocol until the beads were washed. Protein was then eluted by adding PrSc protease to the beads and further purified by Superdex 200 gel filtration.

Protein Labeling—Proteins were labeled with Alexa dyes using commercially available labeling kits (Alexa-488 and Alexa-647 protein labeling kits from Invitrogen).

Co-sedimentation Assays—Liposomes had the same composition as GUVs excluding rhodamine-PE. Lipids were mixed and dried under a stream of argon. To get rid of the remaining solvents, lipids were desiccated for 2 h. Buffer was added to give a final concentration of 1 mg/ml liposomes. Liposomes were re-hydrated for 1 h followed by five freeze-thaw cycles. Liposomes were extruded 21 times through a 100-nm filter (Nucleopore, Track-Etch, Whatman) and used immediately. Liposomes were incubated with 1 μM of the protein(s) indicated in the figures. After 20 min at 37 °C, the liposomes were centrifuged at 150,000 × *g* for 20 min. Supernatants and pellets were separated, and equal amounts of each were loaded onto an SDS gel.

RESULTS AND DISCUSSION

Mutual Recruitment of Dynamin and BAR Domain Proteins in Live Cells—The role of BAR domain proteins thought to recruit dynamin to clathrin-coated pits was assessed in a genome-edited skin fibroblast cell line (SK-MEL-2) having all endogenous clathrin and dynamin2 molecules tagged with red fluorescent protein and eGFP, respectively (28). Depletion of amphiphysin (Amph1+2) by RNA interference (RNAi) led to an increased and prolonged dynamin recruitment to the plasma membrane (Fig. 1, *A–C*). The increased dynamin recruitment is consistent with the known action of amphiphysin in preventing dynamin assembly into larger structures *in vitro* (13). The result also implies that other proteins in addition to amphiphysin are involved in dynamin recruitment. Consistently, amphiphysin RNAi led to defective CME as measured by transferrin (Tf) uptake (Fig. 1, *D* and *E*). This strong dependence of CME on amphiphysin is in line with *Saccharomyces cerevisiae* amphiphysin homologues, with Rvs164/167 being important for endocytosis and observed on the necks of endocytic structures (31, 32). The severity is less consistent with the weak endocytic phenotype of knock-out (KO) mice for amphiphysin1, where amphiphysin2 expression levels are seen to be concomitantly decreased and where synaptic vesicle recycling defects are only observed with strong stimulations (33). However, residual amphiphysin2 in these mice is likely to be functional.

Endophilin is also proposed to be involved in dynamin recruitment to the plasma membrane. Depletion of endophilin (EndoA1+2+3) induced a small decrease in dynamin recruitment, a slight increase in dynamin lifetime at clathrin-coated pits, but no significant decrease in Tf uptake (Fig. 1, *B–E,* and supplemental Fig. S1*A*). Consistent with the observation that SNX9 is recruited after dynamin, endophilin, and amphiphysin (27), RNAi of SNX9 did not result in detectable changes in dynamin levels at the plasma membrane nor in Tf uptake decrease (Fig. 1, *A–E,* and supplemental Fig. S1*A*), and thus it is unlikely to mediate dynamin recruitment at clathrin-coated pits.

The concomitant knockdown of both endophilin and amphiphysin, however (EndoA1+2+3 + Amph1+2 RNAi, supplemental Fig. S2), induced a significant diminution of dynamin recruitment to the plasma membrane (Fig. 1, *A* and *B*) as well as a marked reduction in Tf uptake (Fig. 1, *D* and *E*). Although overexpression of individual full-length BAR+SH3 domain proteins promoted dynamin recruitment to membranes in cells (Fig. 1, *F* and *G,* and supplemental Fig. S1*B*), a significant reduction of dynamin recruitment required the depletion of multiple proteins, implying redundancy between them (Fig. 1*B*).

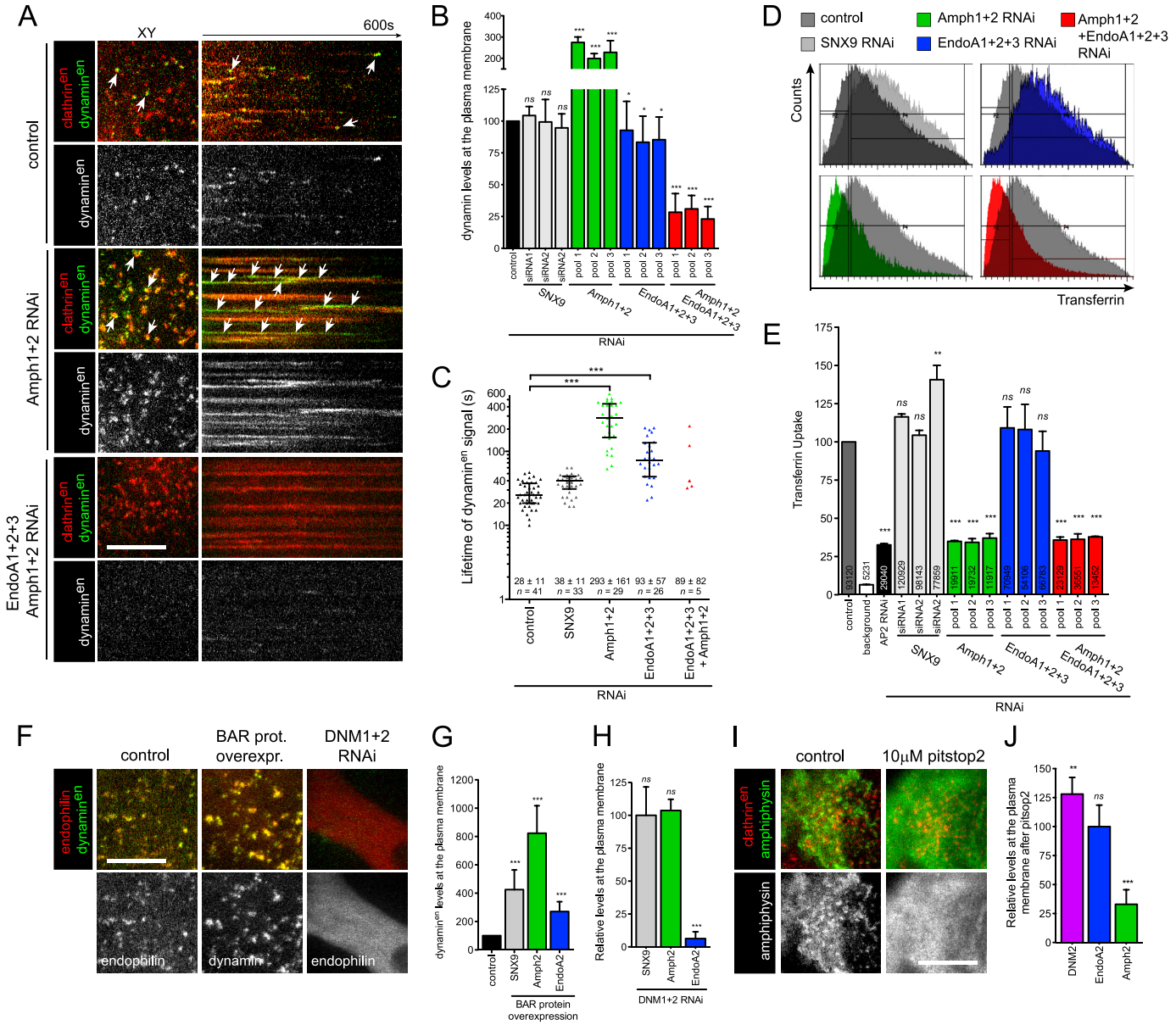

FIGURE 1. **Recruitment of dynamin and of BAR domain proteins in live cells.** *A,* effect of amphiphysin (*Amph1+2 RNAi*) and endophilin + amphiphysin (*EndoA1+2+3 + Amph1+2 RNAi*) depletion on recruitment of endogenous dynamin2 (*dynamin^en*, *green*, see *white arrows*) and clathrin light chain A (*clathrin^en*, *red*). *Bar,* 10 μm. *B,* recruitment of endogenous dynamin at the plasma membrane in cells depleted with three independent pools of siRNA against SNX9 (*gray bars*), amphiphysin (*green bars*), endophilin (*blue bars*), and endophilin + amphiphysin (*red bars*). *C,* scatter plots of individual lifetimes of endogenous dynamin2 from three different cells, measured on dataset similar to *A* and S1A. The median with its interquartile range is shown (*black lines*), and the mean ± S.D. is written at the bottom; *n* is the number of events analyzed. *D,* representative FACS profiles of Tf uptake in cells treated with the indicated siRNA. *E,* effect of the indicated siRNA on transferrin uptake measured by flow cytometry. AP2 depletion was used as positive control (*black bar*). The background (cells without Tf) is shown (*white bar*). The number of cells analyzed is displayed on each bar. *F,* effect of endophilin overexpression on endogenous dynamin recruitment and of dynamin depletion (*DNM1+2 RNAi*) on endophilin recruitment. *Bar,* 10 μm. *G,* recruitment of endogenous dynamin at the plasma membrane in cells overexpressing SNX9 (*gray bar*), amphiphysin (*green bar*), or endophilin (*blue bar*) measured on datasets similar to *F* and supplemental Fig. S1*B*. *H,* recruitment of SNX9 (*gray bar*), amphiphysin (*green bar*) and endophilin (*blue bar*) in cells depleted of dynamin (*DNM1+2 RNAi*) measured on datasets similar to *F* and supplemental Fig. S1*B*. *I,* effect of 10 μM pitstop2 on amphiphysin recruitment at the plasma membrane. The *control* and *10 μM pitstop2* images were taken just before and 5 min after addition of the drug, respectively. *Bar,* 10 μm. *J,* recruitment of dynamin (*magenta bar*), endophilin (*blue bar*), and amphiphysin (*green bar*) in cells treated with 10 μM pitstop2 for 5 min, measured on datasets similar to *I* and supplemental Fig. S1*D*. In *B, E, G, H,* and *J,* the values were normalized to the respective means of the control cells; *ns*, nonsignificant; *, $p < 0.01$; **, $p < 0.001$; ***, $p < 0.0001$.

Given the altered dynamin recruitment with BAR protein depletion, we asked if the plasma membrane localization of BAR+SH3 domain-containing proteins could be altered by decreased dynamin levels. When testing BAR domain protein recruitment to the plasma membrane upon dynamin depletion (DNM1+2 RNAi), we saw that amphiphysin and SNX9 recruitment was unchanged (Fig. 1*H* and supplemental Fig. S1*B*), consistent with their additional binding to AP2 and clathrin through their middle domains (11, 23). In the case of amphiphysin, these interactions have been shown to mediate recruitment, as mutations of this region (11, 34) or acute perturbation of its interaction with clathrin using the small molecule pitstop2 (35) were enough to render the protein cytosolic (Fig. 1, *I* and *J,* and supplemental Fig. S1*D*). Pitstop2 had no

effect on endophilin recruitment (Fig. 1*J* and supplemental Fig. S1*D*). Neither RNAi of amphiphysin nor addition of pitstop2 prevents dynamin recruitment to sites of CME (Fig. 1, *B* and *J*), yet in both cases the lack of amphiphysin at clathrin-coated pits does not allow for functional vesicle scission, implying that amphiphysin plays a key role in the precise localization of dynamin and/or its function.

Finally, dynamin depletion led to a clear reduction of endophilin recruitment to the plasma membrane (Fig. 1, *F* and *G*, and supplemental Fig. S1, *B* and *C*). This indicates a degree of cooperativity of dynamin and endophilin binding to the membrane, as endophilin displays no direct clathrin interaction as an alternative means for recruitment. We next asked if we could investigate cooperative recruitment of BAR domain proteins and dynamin to membranes *in vitro*.

Dynamin Recruitment to Membranes Is Facilitated by Endophilin and Amphiphysin—Membrane localization and the assay of CME in cells show a strong relationship between BAR proteins and dynamin. However, to gain a more precise molecular understanding, we developed a system with reduced complexity. We have therefore reconstituted the activities of these proteins on membranes *in vitro*. Membrane binding of endocytic proteins has classically been shown with spin or flotation assays using small unilamellar vesicles. We considered small unilamellar vesicles an inadequate membrane model system to study dynamin recruitment, because dynamin recruitment to small unilamellar vesicles is robust even in the absence of interaction partners (36). This may be due to enhanced polymerization of dynamin on membranes of high curvature (5). Thus, to visualize dynamin recruitment to membranes, we employed GUVs, which present a virtually flat surface at the protein scale. Shortly after the addition of Alexa-488-labeled dynamin, we observed almost no dynamin recruitment to GUVs (Fig. 2*A*, *upper panel*). However, within 30 min, a strong dynamin signal was seen on the membrane (Fig. 2, *A, bottom panel, B* and *C*). This suggested the possibility that GUVs represent a suitable model membrane system to study potential factors involved in dynamin recruitment. Addition of labeled endophilin to the assay accelerated the recruitment of dynamin to GUV membranes (Fig. 2*D*), as seen also in time courses (Fig. 2, *E* and *F*). Co-recruitment experiments with dynamin and amphiphysin showed comparable results (Fig. 2, *G* and *H*), consistent with earlier results showing an increased rate of GTP hydrolysis by dynamin on membranes in the presence of amphiphysin (26). The addition of endophilin not only led to a more efficient membrane binding of dynamin but also to clustering of both proteins on the membrane (Fig. 2*D, arrows,* and supplemental Movie 1). Such protein clusters were not observed in experiments with dynamin alone (Fig. 2*A*) or with dynamin in the presence of amphiphysin (Fig. 4). This observation fits with earlier experiments showing that amphiphysin disassembles dynamin oligomers (13), whereas endophilin more strongly promotes dynamin assembly (20). From these initial experiments, we conclude that BAR+SH3 proteins promote a more efficient recruitment of dynamin to membranes, and given the variety of these proteins, with various membrane specificities, this should facilitate specific dynamin recruitment to many different membrane scission events.

Endophilin and Amphiphysin Recruitment to Membranes Depends on the PRD of Dynamin—Surprisingly, when changing the order of protein addition, we did not detect the recruitment of full-length endophilin to membranes in the absence of dynamin (Fig. 3*A*). This is similar to our observation in cells where RNAi of dynamin led to a reduced recruitment of endophilin (Fig. 1, *D* and *F*). The *in vitro* system allowed this to be further probed. The N-BAR module alone of endophilin was efficiently recruited (Fig. 3*B*), ruling out any potential interference of protein and lipid labeling with membrane binding and implying that membrane binding of full-length endophilin is auto-inhibited by its cognate SH3 domain. Addition of endophilin N-BAR in many cases also led to visible tubulation of GUVs (Fig. 4*A*). When dynamin was added to full-length endophilin, both proteins were recruited to GUV membranes within seconds (Fig. 3*C*). To further test for auto-inhibition, we performed a series of co-sedimentation assays with SUVs (Fig. 3*D*). Endophilin N-BAR domain efficiently bound to SUVs, as expected, whereas membrane binding was decreased for full-length endophilin. Almost complete membrane binding was restored in the presence of dynamin PRD (Fig. 3*D*) that is known to bind to the SH3 domain of endophilin (10). It is tempting to speculate that the stronger membrane binding of full-length endophilin to SUVs might be due to the higher curvature of the small vesicles serving as a binding template or to an increased membrane tension of the GUVs due to the high sucrose concentration within the vesicles.

On GUVs, the addition of dynamin lacking its PRD (dynaminΔPRD) did not induce endophilin membrane binding, although full-length dynamin did (Fig. 3*E, top* and *middle panels*). Addition of the PRD from dynamin was sufficient to restore endophilin membrane binding, demonstrating that occupying the SH3 domain of endophilin can reverse its auto-inhibited state.

To investigate if this is a general mechanism to regulate membrane binding of N-BAR domain proteins, we performed a similar set of experiments with amphiphysin (Fig. 4), and we found the same regulatory mechanism.

Membrane recruitment of dynamin and endophilin/amphiphysin is thus observed to be cooperative. Dynamin needs a critical concentration for self-polymerization. This can be artificially achieved by increasing the strength of this interaction (low ionic strength buffers) or by using negatively charged membranes with high curvature as a template (36, 37). In a more physiological context, N-BAR domains can likely cooperate with dynamin to make a template for assembly, and in addition, the BAR domain of amphiphysin/endophilin will form a strong dimer in the context of membranes, thus providing two SH3 domains for recruiting dynamin dimers, providing a significant dynamin affinity for relieving the auto-inhibition of the amphiphysin in the first place.

The involvement of SH3 domains in the regulation of amphiphysin, endophilin, and syndapin (also called pacsin) has been noted previously (38, 39). For endophilin and amphiphysin, cognate SH3 domains are proposed to form intramolecular interaction with proline-rich sequences between the BAR and SH3 domains. For pacsins, the BAR domain is suggested as the site of SH3 binding (39), but a functional consequence on mem-

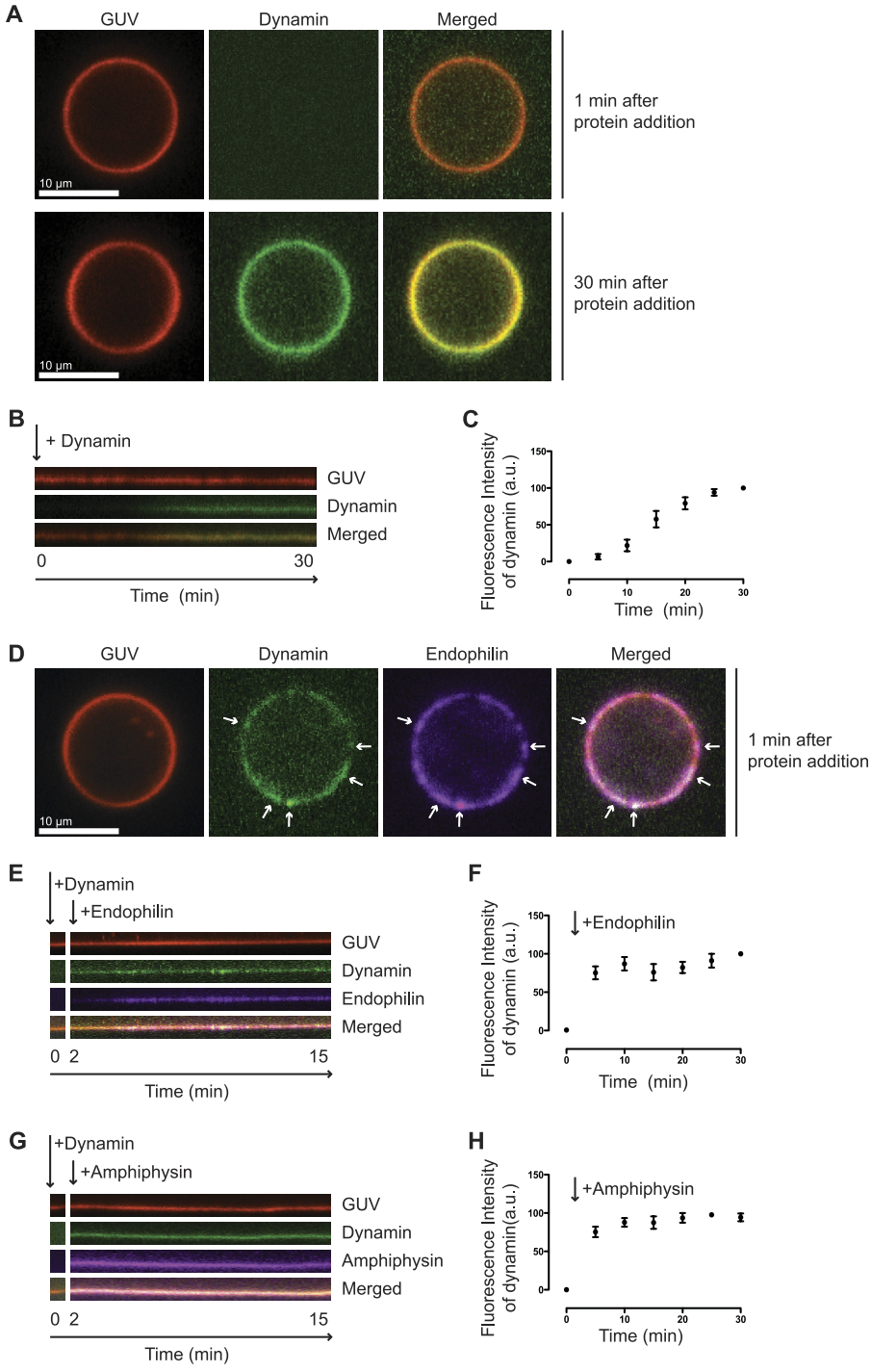

FIGURE 2. **Dynamin recruitment to membranes is facilitated by endophilin.** GUVs (*red*) were labeled with rhodamine-PE; dynamin (*green*) was labeled with Alexa-488, and endophilin (*blue*) was labeled with Alexa-647. Protein concentrations are 300 nm dynamin and 500 nm endophilin/amphiphysin. *A,* GUV in the presence of dynamin 1 min after protein addition (*top panel*) and 30 min after protein addition (*bottom panel*). *B,* kymograph showing one particular area of the GUV over 30 min starting immediately after the addition of dynamin. *C,* normalized fluorescence intensity of dynamin on the GUV. *D,* GUV in the presence of dynamin and endophilin 1 min after protein addition. *E,* kymograph showing one particular area of the GUV over 15 min. Dynamin was added just before the beginning of the kymograph, and endophilin was added 2 min later. *F,* normalized fluorescence intensity of dynamin on the GUV. *G,* kymograph over 15 min. Dynamin was added just before the beginning of the kymograph, and amphiphysin was added 2 min later. *H,* normalized fluorescence intensity of dynamin on the GUV.

brane binding was not uncovered. Here, we establish for endophilin and amphiphysin that their SH3 domains directly inhibit membrane binding, pointing to the BAR domain as the most likely site for the SH3 interaction. In addition, we show that the N-BAR domain alone of endophilin recapitulates the binding of full-length endophilin + the PRD of dynamin. The exact site of this interaction has not been mapped in this study.

Endophilin and Amphiphysin Increase Dynamin and GTP-dependent Vesicle Release from GUVs—Different models for membrane scission by dynamin exist. The two published

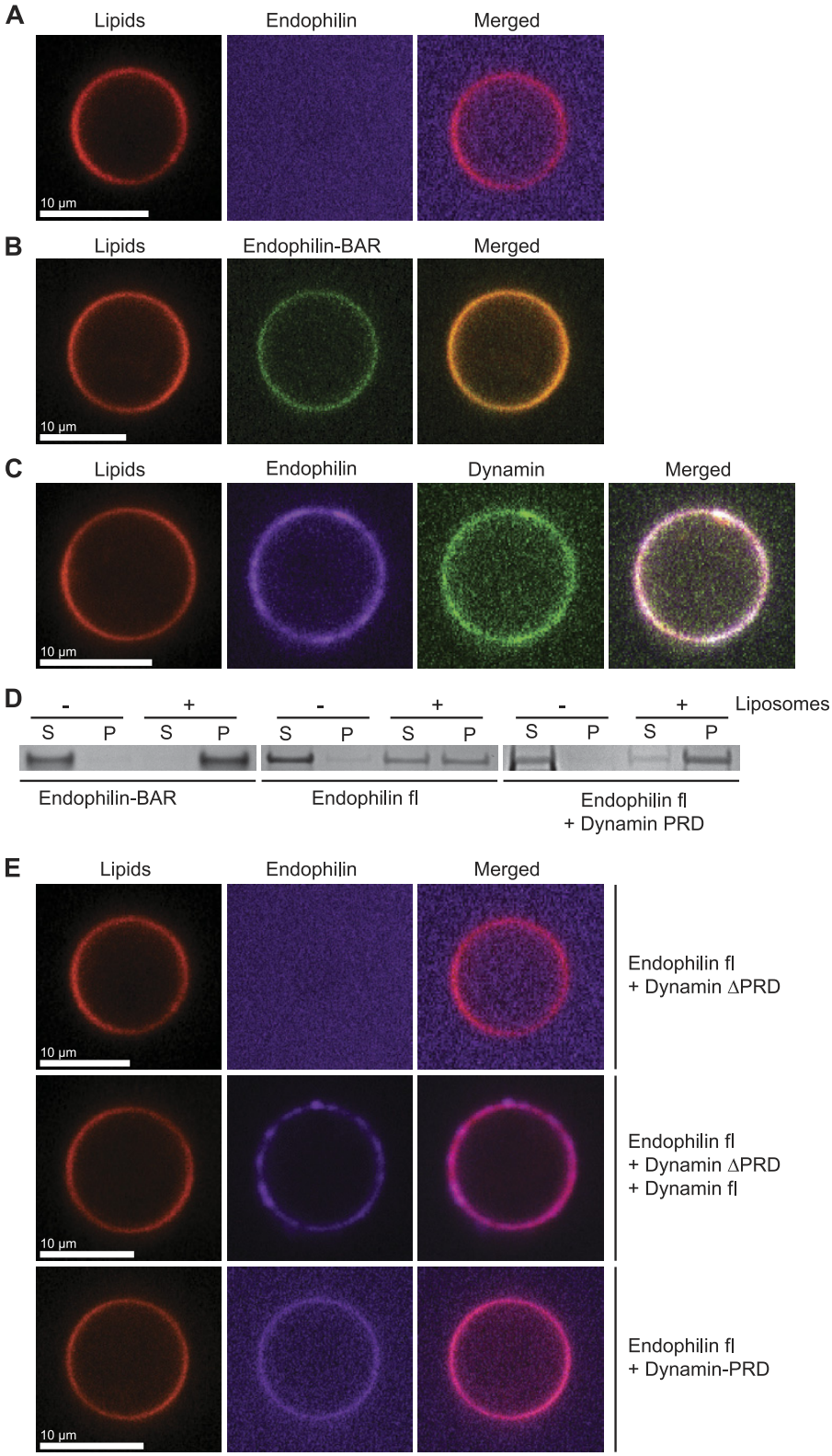

FIGURE 3. **Endophilin recruitment to membranes depends on the PRD of dynamin.** GUVs and protein labeled as in Fig. 2. Endophilin N-BAR domain (*green*) was labeled with Alexa-488. *A,* GUV in the presence of 1 μM full-length endophilin. *B,* GUV in the presence of 1 μM endophilin N-BAR domain. *C,* GUV in the presence of 500 nM full-length endophilin and 300 nM dynamin. *D,* liposome sedimentation assay in the presence of endophilin-N-BAR (*left panel*), endophilin full-length (*fl*) (*middle panel*), and endophilin full-length plus the PRD of dynamin. *S* is supernatant, and *P* is pellet. *E,* GUV in the presence of 1 μM endophilin plus 1 μM dynamin-ΔPRD (*top panel*), 1 μM endophilin plus 1 μM dynamin-ΔPRD plus 500 nM full-length dynamin (*middle panel*), and 1 μM endophilin plus 2 μM PRD (*bottom panel*).

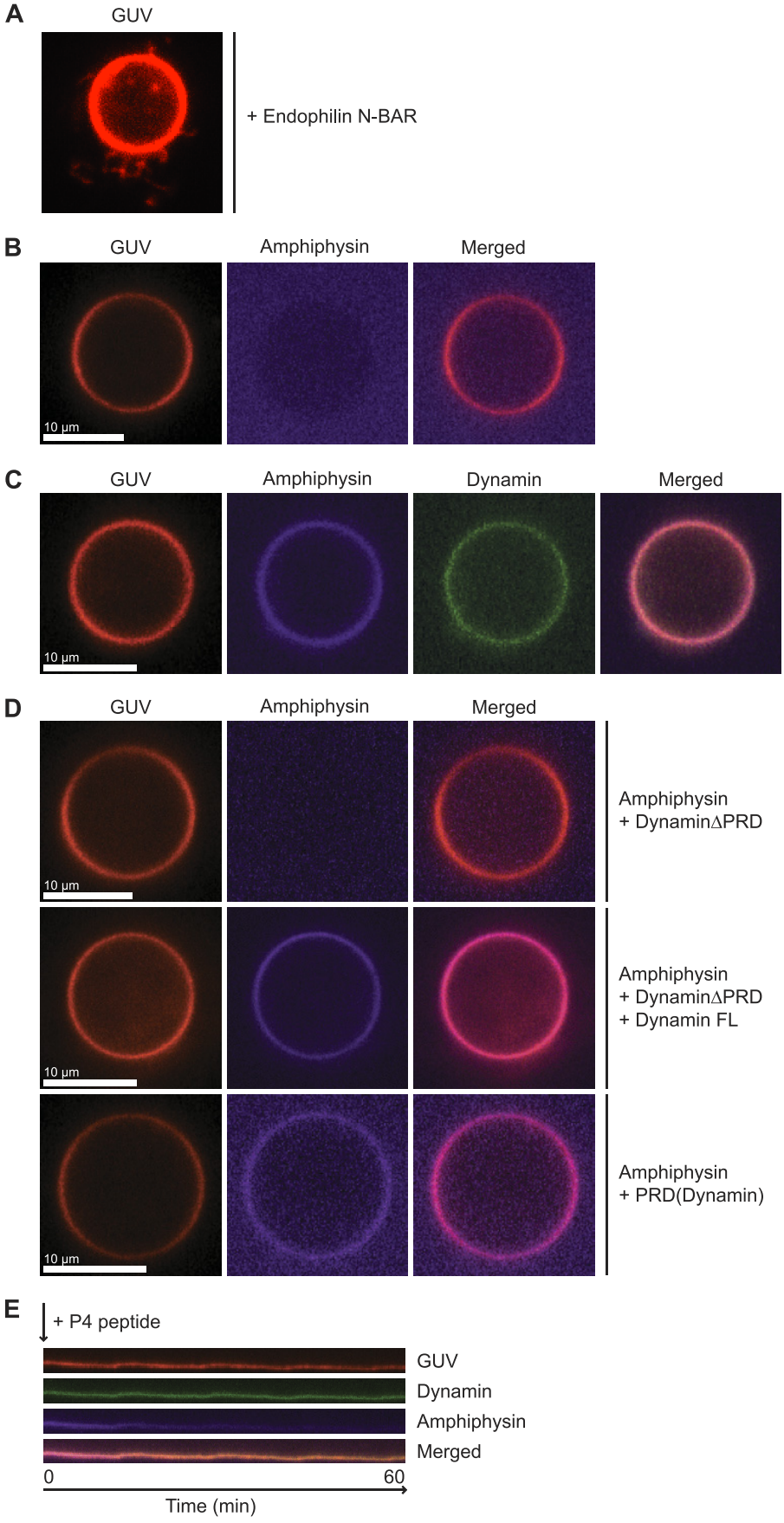

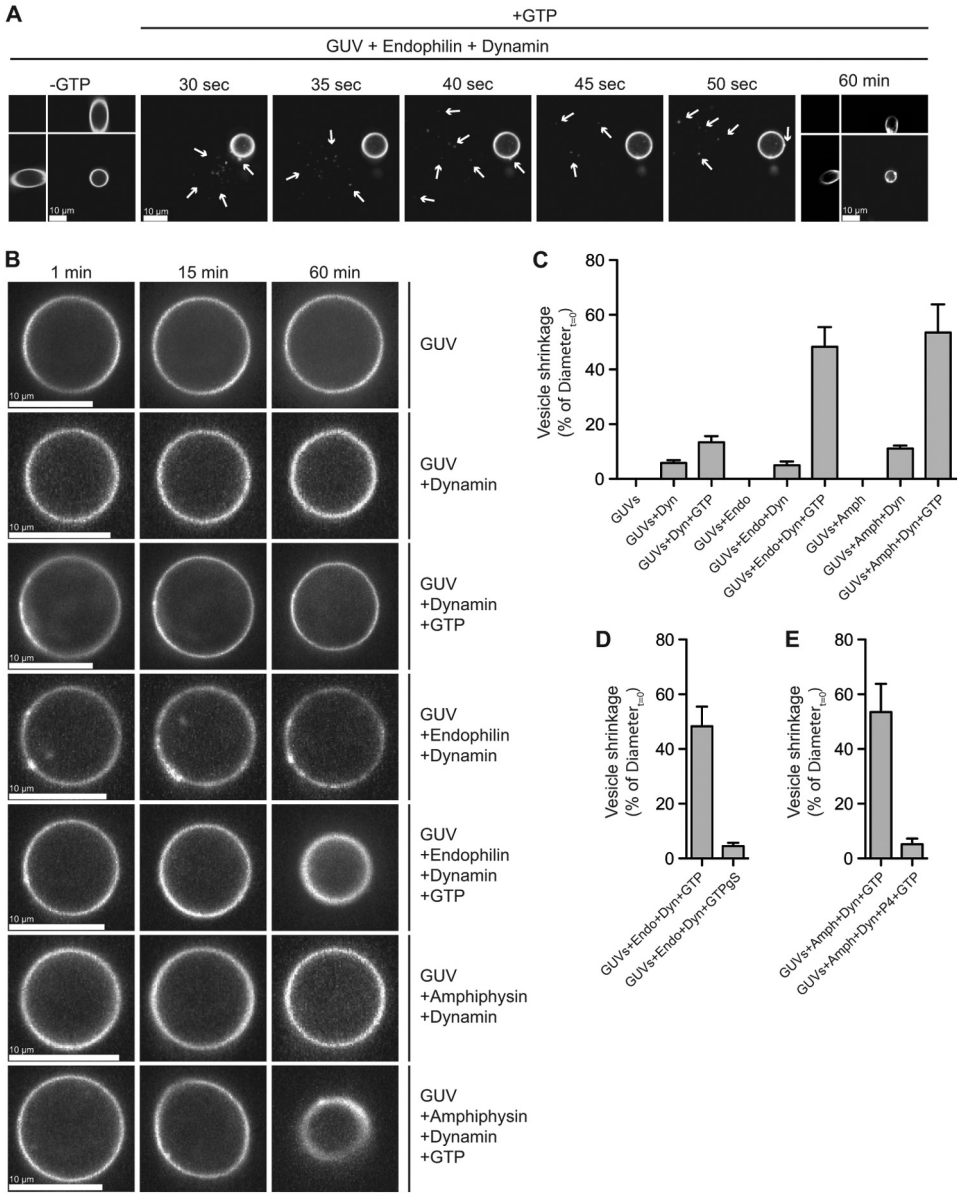

FIGURE 5. **GTP-dependent vesicle release leads to shrinkage of parent GUVs.** GUVs and protein labeled as in Fig. 3. *A,* time course of a GUV with bound dynamin and endophilin in the absence (*−GTP*) and presence of GTP. *Z*-stacks (*−GTP* and *60 min*) show volume shrinkage of the GUV. *B,* time course of GUV shrinkage under the indicated conditions. *C,* quantitation of time courses of at least five independent vesicle preparations (mean with S.E.). *D,* quantitation of the vesiculation in the presence of GTPγS. *E,* quantitation of vesiculation in the presence of a peptide (P4) that disrupts the amphiphysin-dynamin interaction. Vesicle shrinkage was calculated according to $(D_0 - D_{60}) \times 100/D_0$. D_{60} is the vesicle diameter after 60 min, and D_0 is the vesicle diameter at the beginning of the experiment.

dynamin structures propose a mechanism of how GTP hydrolysis could be coupled to membrane scission (40, 41), and a very recently published model is taking physical parameters of the membrane into account (42). Although our assay does not allow us to test for possible scission mechanisms, we can ask the following question. What is the likely consequence of cooperative membrane binding on dynamin-dependent membrane scission? It has been shown in the past that dynamin is sufficient to release small vesicles from membrane templates in a GTP-dependent manner (6, 43), and dynamin is capable of causing scission of membrane tethers (44, 45). Using GUVs, we observed that addition of dynamin resulted in sporadic tubular structures on the vesicle surfaces and that those structures were released in response to GTP addition (results not shown). However, these events were rather infrequent, and thus we asked if we would see a difference in the presence of BAR domain proteins. In the presence of dynamin and endophilin, GUVs were stable for hours (Fig. 5*A, −GTP*). However, subsequent addi-

FIGURE 4. **Amphiphysin recruitment to membranes depends on the PRD of dynamin.** GUVs (*red*) were labeled with rhodamine-PE; dynamin (*green*) was labeled with Alexa-488; amphiphysin (*blue*) was labeled with Alexa-647. *A,* GUV in the presence of 1 μM endophilin N-BAR domain. *B,* GUV in the presence of 1 μM amphiphysin. *C,* GUV in the presence of 500 nM amphiphysin and 300 nM dynamin. *D,* GUV in the presence of 1 μM amphiphysin plus 1 μM dynamin-ΔPRD (*top panel*), 1 μM amphiphysin plus 1 μM dynamin-ΔPRD plus 500 nM full-length dynamin (*middle panel*), and 1 μM amphiphysin plus 2 μM PRD (*bottom panel*). *E,* kymograph showing one particular area of a GUV loaded with dynamin and amphiphysin over 60 min. 25 μM P4 peptide, which disrupts the amphiphysin and dynamin interaction, was added at the beginning of the measurement.

tion of GTP led to a visible release of small vesicles from the GUVs (Fig. 5*A, arrows*). Following the same GUV over a longer period of time revealed a significant volume reduction (Fig. 5*A, 60 min*), most likely due to the continuous release of small vesicles and the consumption of the GUV.

Because it was neither possible to reliably quantify by microscopy the number and rate of released vesicles nor to separate or purify them biochemically from the rather fragile GUVs, we used the GUV shrinkage rate as a robust readout of vesiculation under different conditions (Fig. 5, *B* and *C*). GUVs alone were stable for hours. After incubation with dynamin for 30 min (to allow for the slow recruitment), we observed sporadic tubules on GUVs, which over time led to marginal changes of the GUV diameter. The addition of GTP to membrane-bound dynamin resulted in some vesicle release and a minor shrinkage of GUVs (Fig. 5, *B* and *C, GUV+Dyn+GTP*). The GUV shrinkage was dramatically increased if GTP was added to vesicles loaded with dynamin and either endophilin or amphiphysin (Fig. 5, *B* and *C*). Addition of GTPγS did not lead to visible changes (Fig. 5*D*). We conclude that amphiphysin and endophilin promote GTP-dependent membrane scission. Assuming the release of 10-nm vesicles, a decrease in the GUV diameter from 10 to 5 μm over 60 min will result from the release of between 5000 and 10,000 vesicles, or at least 1–2 vesicles/s.

To ask if the promotion of membrane scission is a result of enhanced recruitment or if the BAR protein may be participating in the scission event, we used a small peptide inhibitor of dynamin-amphiphysin interactions. The P4 peptide is derived from the amphiphysin-binding site in dynamin (sequence, QVPSRPNRAP) (4, 13) and has been used in cells to disrupt endocytic activity (46, 47). Addition of P4 caused the release of amphiphysin (bound in the presence of dynamin) from GUVs, but the dynamin signal was not diminished (Fig. 4*D*). GUVs now showed no shrinkage after GTP addition (Fig. 5*E*), showing that vesicle scission is dependent on the presence of all three components, dynamin, GTP, and amphiphysin.

Our results show that N-BAR proteins are indeed necessary for dynamin recruitment and activity. We propose that both the enhanced recruitment and the regulation of dynamin activity in the presence of N-BAR proteins explain the importance of these proteins *in vivo*. We see that depletion of amphiphysin or blocking its recruitment to clathrin-coated pits are both effective ways to inhibit CME. The inhibition of amphiphysin recruitment observed upon treatment with pitstop2, a small molecule previously shown to inhibit CME (35), points to the importance of amphiphysin in membrane scission and in the regulation of dynamin activity.

Our results are consistent with a view of CME as a network of interactions where the membrane scission molecule, dynamin, is recruited by proteins that themselves aid in making the neck template and in addition are synergistically regulated by dynamin.

Acknowledgments—We thank Patricia Bassereau for advice concerning the generation of GUVs. We thank David Drubin, Volker Haucke, and Safa Lucken-Ardjomande for kindly providing the genome-edited cells, pitstop2, and amphiphysin constructs for live-cell imaging, respectively.

REFERENCES

1. McMahon, H. T., and Boucrot, E. (2011) Molecular mechanism and physiological functions of clathrin-mediated endocytosis. *Nat. Rev. Mol. Cell Biol.* **12,** 517–533
2. Gout, I., Dhand, R., Hiles, I. D., Fry, M. J., Panayotou, G., Das, P., Truong, O., Totty, N. F., Hsuan, J., Booker, G. W., *et al.* (1993) The GTPase dynamin binds to and is activated by a subset of SH3 domains. *Cell* **75,** 25–36
3. Shpetner, H. S., Herskovits, J. S., and Vallee, R. B. (1996) A binding site for SH3 domains targets dynamin to coated pits. *J. Biol. Chem.* **271,** 13–16
4. Grabs, D., Slepnev, V. I., Songyang, Z., David, C., Lynch, M., Cantley, L. C., and De Camilli, P. (1997) The SH3 domain of amphiphysin binds the proline-rich domain of dynamin at a single site that defines a new SH3 binding consensus sequence. *J. Biol. Chem.* **272,** 13419–13425
5. Roux, A., Koster, G., Lenz, M., Sorre, B., Manneville, J. B., Nassoy, P., and Bassereau, P. (2010) Membrane curvature controls dynamin polymerization. *Proc. Natl. Acad. Sci. U.S.A.* **107,** 4141–4146
6. Sweitzer, S. M., and Hinshaw, J. E. (1998) Dynamin undergoes a GTP-dependent conformational change causing vesiculation. *Cell* **93,** 1021–1029
7. Peter, B. J., Kent, H. M., Mills, I. G., Vallis, Y., Butler, P. J., Evans, P. R., and McMahon, H. T. (2004) BAR domains as sensors of membrane curvature: the amphiphysin BAR structure. *Science* **303,** 495–499
8. Gallop, J. L., Jao, C. C., Kent, H. M., Butler, P. J., Evans, P. R., Langen, R., and McMahon, H. T. (2006) Mechanism of endophilin N-BAR domain-mediated membrane curvature. *EMBO J.* **25,** 2898–2910
9. David, C., McPherson, P. S., Mundigl, O., and de Camilli, P. (1996) A role of amphiphysin in synaptic vesicle endocytosis suggested by its binding to dynamin in nerve terminals. *Proc. Natl. Acad. Sci. U.S.A.* **93,** 331–335
10. Ringstad, N., Nemoto, Y., and De Camilli, P. (1997) The SH3p4/Sh3p8/SH3p13 protein family. Binding partners for synaptojanin and dynamin via a Grb2-like Src homology 3 domain. *Proc. Natl. Acad. Sci. U.S.A.* **94,** 8569–8574
11. McMahon, H. T., Wigge, P., and Smith, C. (1997) Clathrin interacts specifically with amphiphysin and is displaced by dynamin. *FEBS Lett.* **413,** 319–322
12. Wigge, P., Vallis, Y., and McMahon, H. T. (1997) Inhibition of receptor-mediated endocytosis by the amphiphysin SH3 domain. *Curr. Biol.* **7,** 554–560
13. Owen, D. J., Wigge, P., Vallis, Y., Moore, J. D., Evans, P. R., and McMahon, H. T. (1998) Crystal structure of the amphiphysin-2 SH3 domain and its role in the prevention of dynamin ring formation. *EMBO J.* **17,** 5273–5285
14. Shupliakov, O., Löw, P., Grabs, D., Gad, H., Chen, H., David, C., Takei, K., De Camilli, P., and Brodin, L. (1997) Synaptic vesicle endocytosis impaired by disruption of dynamin-SH3 domain interactions. *Science* **276,** 259–263
15. Simpson, F., Hussain, N. K., Qualmann, B., Kelly, R. B., Kay, B. K., McPherson, P. S., and Schmid, S. L. (1999) SH3-domain-containing proteins function at distinct steps in clathrin-coated vesicle formation. *Nat. Cell Biol.* **1,** 119–124
16. Verstreken, P., Kjaerulff, O., Lloyd, T. E., Atkinson, R., Zhou, Y., Meinertzhagen, I. A., and Bellen, H. J. (2002) Endophilin mutations block clathrin-mediated endocytosis but not neurotransmitter release. *Cell* **109,** 101–112
17. Schuske, K. R., Richmond, J. E., Matthies, D. S., Davis, W. S., Runz, S., Rube, D. A., van der Bliek, A. M., and Jorgensen, E. M. (2003) Endophilin is required for synaptic vesicle endocytosis by localizing synaptojanin. *Neuron* **40,** 749–762
18. Gad, H., Ringstad, N., Löw, P., Kjaerulff, O., Gustafsson, J., Wenk, M., Di Paolo, G., Nemoto, Y., Crun, J., Ellisman, M. H., De Camilli, P., Shupliakov, O., and Brodin, L. (2000) Fission and uncoating of synaptic clathrin-coated vesicles are perturbed by disruption of interactions with the SH3 domain of endophilin. *Neuron* **27,** 301–312
19. Ferguson, S. M., Ferguson, S., Raimondi, A., Paradise, S., Shen, H., Mesaki, K., Ferguson, A., Destaing, O., Ko, G., Takasaki, J., Cremona, O., O' Toole E., and De Camilli, P. (2009) Coordinated actions of actin and BAR proteins upstream of dynamin at endocytic clathrin-coated pits. *Dev. Cell* **17,** 811–822
20. Sundborger, A., Soderblom, C., Vorontsova, O., Evergren, E., Hinshaw,

J. E., and Shupliakov, O. (2011) An endophilin-dynamin complex promotes budding of clathrin-coated vesicles during synaptic vesicle recycling. *J. Cell Sci.* **124,** 133–143
21. Farsad, K., Ringstad, N., Takei, K., Floyd, S. R., Rose, K., and De Camilli, P. (2001) Generation of high curvature membranes mediated by direct endophilin bilayer interactions. *J. Cell Biol.* **155,** 193–200
22. Takei, K., Slepnev, V. I., Haucke, V., and De Camilli, P. (1999) Functional partnership between amphiphysin and dynamin in clathrin-mediated endocytosis. *Nat. Cell Biol.* **1,** 33–39
23. Lundmark, R., and Carlsson, S. R. (2003) Sorting nexin 9 participates in clathrin-mediated endocytosis through interactions with the core components. *J. Biol. Chem.* **278,** 46772–46781
24. Soulet, F., Yarar, D., Leonard, M., and Schmid, S. L. (2005) SNX9 regulates dynamin assembly and is required for efficient clathrin-mediated endocytosis. *Mol. Biol. Cell* **16,** 2058–2067
25. Wigge, P., Köhler, K., Vallis, Y., Doyle, C. A., Owen, D., Hunt, S. P., and McMahon, H. T. (1997) Amphiphysin heterodimers: potential role in clathrin-mediated endocytosis. *Mol. Biol. Cell* **8,** 2003–2015
26. Yoshida, Y., Kinuta, M., Abe, T., Liang, S., Araki, K., Cremona, O., Di Paolo, G., Moriyama, Y., Yasuda, T., De Camilli, P., and Takei, K. (2004) The stimulatory action of amphiphysin on dynamin function is dependent on lipid bilayer curvature. *EMBO J.* **23,** 3483–3491
27. Taylor, M. J., Perrais, D., and Merrifield, C. J. (2011) A high precision survey of the molecular dynamics of mammalian clathrin-mediated endocytosis. *PLoS Biol.* **9,** e1000604
28. Doyon, J. B., Zeitler, B., Cheng, J., Cheng, A. T., Cherone, J. M., Santiago, Y., Lee, A. H., Vo, T. D., Doyon, Y., Miller, J. C., Paschon, D. E., Zhang, L., Rebar, E. J., Gregory, P. D., Urnov, F. D., and Drubin, D. G. (2011) Rapid and efficient clathrin-mediated endocytosis revealed in genome-edited mammalian cells. *Nat. Cell Biol.* **13,** 331–337
29. Henne, W. M., Boucrot, E., Meinecke, M., Evergren, E., Vallis, Y., Mittal, R., and McMahon, H. T. (2010) FCHo proteins are nucleators of clathrin-mediated endocytosis. *Science* **328,** 1281–1284
30. Angelova, M. I., and Dimitrov, D. S. (1986) *Faraday Discuss.* **81,** 303
31. Lombardi, R., and Riezman, H. (2001) Rvs161p and Rvs167p, the two yeast amphiphysin homologs, function together *in vivo*. *J. Biol. Chem.* **276,** 6016–6022
32. Kaksonen, M., Toret, C. P., and Drubin, D. G. (2005) A modular design for the clathrin- and actin-mediated endocytosis machinery. *Cell* **123,** 305–320
33. Di Paolo, G., Sankaranarayanan, S., Wenk, M. R., Daniell, L., Perucco, E., Caldarone, B. J., Flavell, R., Picciotto, M. R., Ryan, T. A., Cremona, O., and De Camilli, P. (2002) Decreased synaptic vesicle recycling efficiency and cognitive deficits in amphiphysin 1 knockout mice. *Neuron* **33,** 789–804
34. Wang, L. H., Südhof, T. C., and Anderson, R. G. (1995) The appendage domain of α-adaptin is a high affinity binding site for dynamin. *J. Biol. Chem.* **270,** 10079–10083
35. von Kleist, L., Stahlschmidt, W., Bulut, H., Gromova, K., Puchkov, D., Robertson, M. J., MacGregor, K. A., Tomilin, N., Tomlin, N., Pechstein, A., Chau, N., Chircop, M., Sakoff, J., von Kries, J. P., Saenger, W., Kräusslich, H. G., Shupliakov, O., Robinson, P. J., McCluskey, A., and Haucke, V. (2011) Role of the clathrin terminal domain in regulating coated pit dynamics revealed by small molecule inhibition. *Cell* **146,** 471–484
36. Hinshaw, J. E., and Schmid, S. L. (1995) Dynamin self-assembles into rings suggesting a mechanism for coated vesicle budding. *Nature* **374,** 190–192
37. Stowell, M. H., Marks, B., Wigge, P., and McMahon, H. T. (1999) Nucleotide-dependent conformational changes in dynamin: evidence for a mechanochemical molecular spring. *Nat. Cell Biol.* **1,** 27–32
38. Chen, Y., Deng, L., Maeno-Hikichi, Y., Lai, M., Chang, S., Chen, G., and Zhang, J. F. (2003) Formation of an endophilin-Ca^{2+} channel complex is critical for clathrin-mediated synaptic vesicle endocytosis. *Cell* **115,** 37–48
39. Rao, Y., Ma, Q., Vahedi-Faridi, A., Sundborger, A., Pechstein, A., Puchkov, D., Luo, L., Shupliakov, O., Saenger, W., and Haucke, V. (2010) Molecular basis for SH3 domain regulation of F-BAR-mediated membrane deformation. *Proc. Natl. Acad. Sci. U.S.A.* **107,** 8213–8218
40. Faelber, K., Posor, Y., Gao, S., Held, M., Roske, Y., Schulze, D., Haucke, V., Noé, F., and Daumke, O. (2011) Crystal structure of nucleotide-free dynamin. *Nature* **477,** 556–560
41. Ford, M. G., Jenni, S., and Nunnari, J. (2011) The crystal structure of dynamin. *Nature* **477,** 561–566
42. Morlot, S., Galli, V., Klein, M., Chiaruttini, N., Manzi, J., Humbert, F., Dinis, L., Lenz, M., Cappello, G., and Roux, A. (2012) Membrane shape at the edge of the dynamin helix sets location and duration of the fission reaction. *Cell* **151,** 619–629
43. Pucadyil, T. J., and Schmid, S. L. (2008) Real-time visualization of dynamin-catalyzed membrane fission and vesicle release. *Cell* **135,** 1263–1275
44. Bashkirov, P. V., Akimov, S. A., Evseev, A. I., Schmid, S. L., Zimmerberg, J., and Frolov, V. A. (2008) GTPase cycle of dynamin is coupled to membrane squeeze and release, leading to spontaneous fission. *Cell* **135,** 1276–1286
45. Roux, A., Uyhazi, K., Frost, A., and De Camilli, P. (2006) GTP-dependent twisting of dynamin implicates constriction and tension in membrane fission. *Nature* **441,** 528–531
46. Marks, B., and McMahon, H. T. (1998) Calcium triggers calcineurin-dependent synaptic vesicle recycling in mammalian nerve terminals. *Curr. Biol.* **8,** 740–749
47. Nong, Y., Huang, Y. Q., Ju, W., Kalia, L. V., Ahmadian, G., Wang, Y. T., and Salter, M. W. (2003) Glycine binding primes NMDA receptor internalization. *Nature* **422,** 302–307

Supplementary Information

Figure legends

Supplementary Figure 1 | Dynamin and BAR domain proteins recruitment in live cells

(A) Effect of SNX9 (SNX9 RNAi), amphiphysin (Amph1+2 RNAi), endophilin (EndoA1+2+3) and endophilin + amphiphysin (EndoA1+2+3 + Amph1+2 RNAi) depletion on the recruitment of endogenous dynamin 2 (dynamin^{en}, green and white arrows) and clathrin light chain A (clathrin^{en}, red). Bar, 10μm

(B) Effect of SNX9, amphiphysin and endophilin overexpression on endogenous dynamin 2 (dynamin^{en}, green) recruitment and effect of dynamin depletion (DNM1+2 RNAi) on SNX9, amphiphysin and endophilin recruitment. Bar, 10μm

(C) Effect of dynamin depletion (DNM1+2 RNAi) on endogenous endophilin recruitment labelled with antibodies sc25495 or sc10880. Outlines of the knock down cells are shown. Boxed regions are magnified on the right of each image. Bar, 20μm. Two different antibodies have been used as this result is in contradiction with those in dynamin1/2 knockout mice showing an accumulation of endophilin into patches at the plasma membrane (1). Nevertheless differences between knockout mice and transiently affected cells have been noticed before (2,3) and may be due to compensatory effects within a developing organism.

(D) Effect of 10μM pitstop2 on dynamin, endophilin and amphiphysin recruitment at the plasma membrane. The 'control' and '10μM pitstop2' images were taken just before and 5 min after addition of the drug, respectively. Bar, 10μm

Supplementary Figure 2 | Knockdown levels of RNAi treated cells.

Representative cell extracts depleted for (**A**) amphiphysin (Amph1+2 RNAi), endophilin (EndoA1+2+3) and endophilin + amphiphysin (EndoA1+2+3 + Amph1+2 RNAi), (**B**) dynamin (Dynamin1+2 RNAi) or (**C**) SNX9 (SNX9 RNAi) and used in Figure 1 and S1. Proteins were separated by Western blotting and immunoprobed with the indicated antibodies.

Movie 1 | Endophilin and dynamin co-localization on GUVs. The GUV (red) was labelled with rhodamine-PE, dynamin (green) was labelled with Alexa488 and endophilin (blue) was labelled with Alexa647. Slight mismatches in co-localization between dynamin and endophilin are due to high mobility of extremely dynamic protein cluster and the delay in channel switching on the microscope. Movie was sampled at 1Hz and played at 10frames/second. The total length of the movie is 140seconds.

References

1. Ferguson, S. M., Raimondi, A., Paradise, S., Shen, H., Mesaki, K., Ferguson, A., Destaing, O., Ko, G., Takasaki, J., Cremona, O., E, O. T., and De Camilli, P. (2009) *Dev Cell* **17**, 811-822
2. Di Paolo, G., Sankaranarayanan, S., Wenk, M. R., Daniell, L., Perucco, E., Caldarone, B. J., Flavell, R., Picciotto, M. R., Ryan, T. A., Cremona, O., and De Camilli, P. (2002) *Neuron* **33**, 789-804
3. Evergren, E., Marcucci, M., Tomilin, N., Low, P., Slepnev, V., Andersson, F., Gad, H., Brodin, L., De Camilli, P., and Shupliakov, O. (2004) *Traffic* **5**, 514-528
4. Doyon, J. B., Zeitler, B., Cheng, J., Cheng, A. T., Cherone, J. M., Santiago, Y., Lee, A. H., Vo, T. D., Doyon, Y., Miller, J. C., Paschon, D. E., Zhang, L., Rebar, E. J., Gregory, P. D., Urnov, F. D., and Drubin, D. G. (2011) *Nat Cell Biol* **13**, 331-337

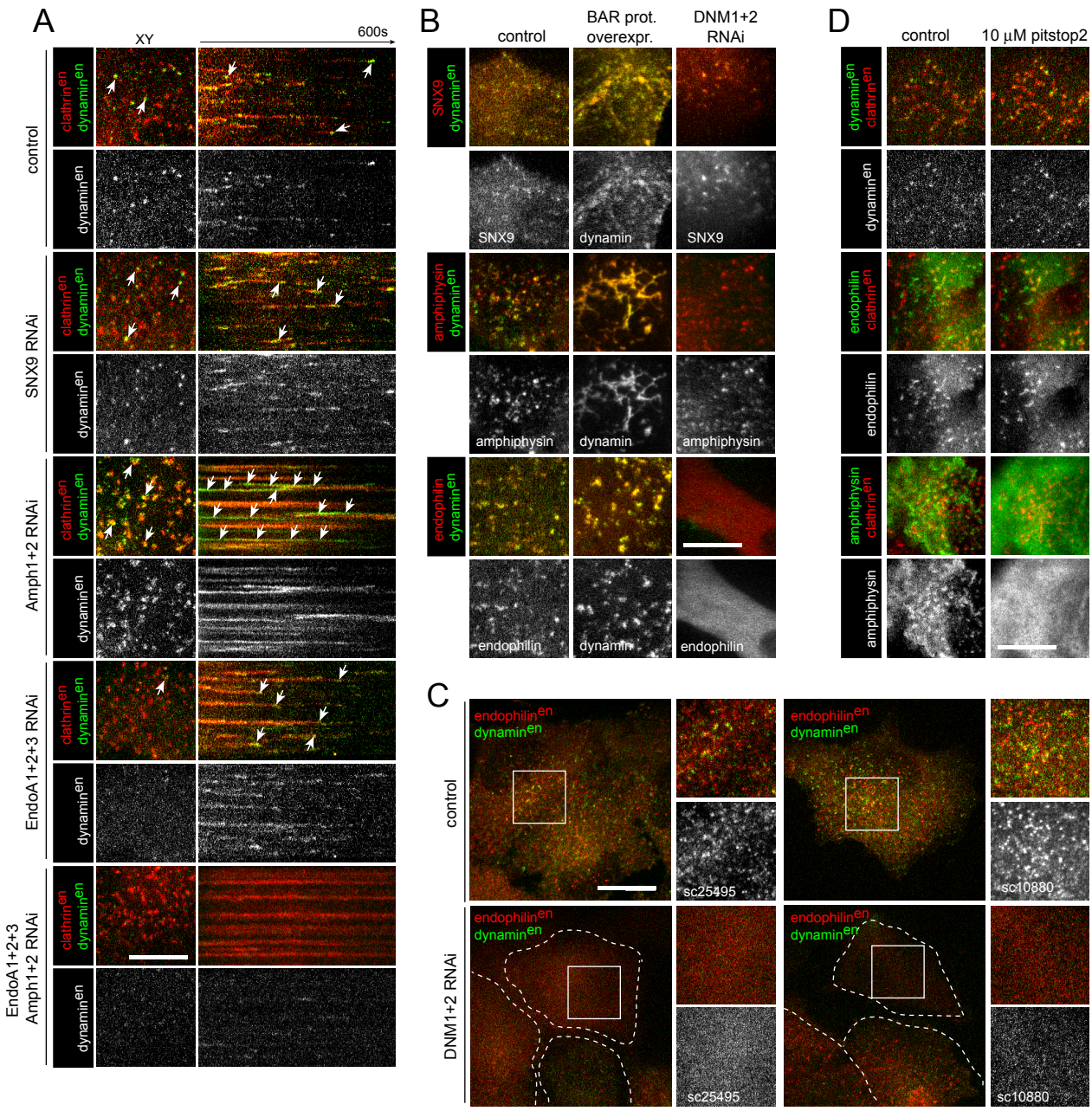

Supplementary Figure 1 Meinecke et al.

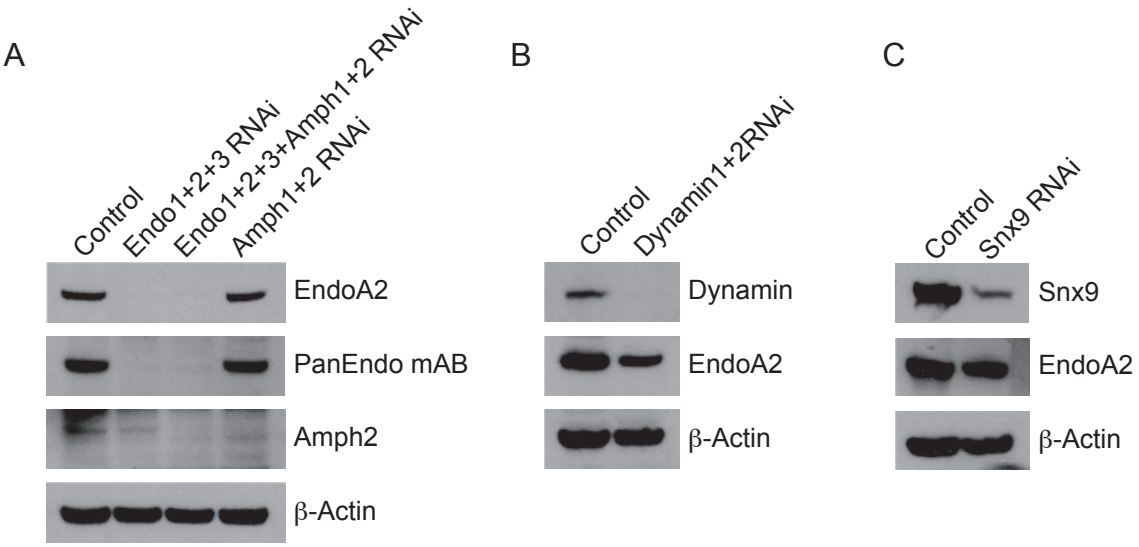

Supplementary Figure 2 Meinecke et al.